The Antiviral Nucleotide Analogs Cidofovir and Adefovir Are Novel Substrates for Human and Rat Renal Organic Anion Transporter 1

TOMAS CIHLAR, DEBORAH C. LIN, JOHN B. PRITCHARD, MICHAEL D. FULLER, DIRK B. MENDEL, and DOUGLAS H. SWEET

Gilead Sciences, Foster City, California (T.C., D.C.L., M.D.F., D.B.M.); and Laboratory of Pharmacology and Chemistry, National Institute of Environmental Health Sciences, Research Triangle Park, North Carolina (J.B.P., D.H.S)

This paper is available online at http://www.molpharm.org

ABSTRACT

Nephrotoxicity is the dose-limiting clinical adverse effect of cidofovir and adefovir, two potent antiviral therapeutics. Because renal uptake likely plays a role in the etiology of cidofovir- and adefovir-associated nephrotoxicity, we attempted to identify a renal transporter capable of interacting with these therapeutics. A cDNA clone was isolated from a human renal library and designated human organic anion transporter 1 (hOAT1). Northern analysis detected a specific 2.5-kilobase pair hOAT1 transcript only in human kidney. However, reverse transcription-polymerase chain reaction revealed hOAT1 expression in human brain and skeletal muscle, as well. Immunoblot analysis of human kidney cortex demonstrated that hOAT1 is an 80- to 90-kilodalton heterogeneous protein modified by abundant N-glycosylation. *Xe-nopus laevis* oocytes expressing hOAT1 supported probenecid-sensitive uptake of [^{3}H]p-aminohippurate ($K_m = 4\ \mu M$), which was *trans*-stimulated in oocytes preloaded with glutarate. Importantly, both hOAT1 and rat renal organic anion transporter 1 (rROAT1) mediated saturable, probenecid-sensitive uptake of cidofovir, adefovir, and other nucleoside phosphonate antivirals. The affinity of hOAT1 toward cidofovir and adefovir ($K_m = 46$ and $30\ \mu M$, respectively) was 5- to 9-fold higher compared with rROAT1 ($K_m = 238$ and $270\ \mu M$, respectively). These data indicate that hOAT1 may significantly contribute to the accumulation of cidofovir and adefovir in renal proximal tubules and, thus, play an active role in the mechanism of nephrotoxicity associated with these antiviral therapeutics.

Successful management of viral infections often requires long-term therapy with highly potent antivirals. However, various adverse effects may be induced by prolonged administration of antiviral drugs. For example, long-term azidothymidine and dideoxycytidine therapy causes myopathy and peripheral neuropathy, respectively, in a number of AIDS patients (Dalakas et al., 1990; Dubinsky et al., 1989). Similarly, extended therapy with HIV protease inhibitors may be associated with peripheral lipodystrophy, hyperlipidemia, and insulin-resistant diabetes (Carr et al., 1998). However, the main dose-limiting clinical factor for cidofovir [(S)-1-(3-hydroxy-2-phosphonylmethoxypropyl)cytosine] and adefovir [9-(2-phosphonylmethoxyethyl)adenine], two potent antiviral agents with unique resistance profiles, is nephrotoxicity

characterized by changes in laboratory markers of renal function (Lalezari et al., 1997; Fisher et al., 1999). Both cidofovir and adefovir are nucleoside phosphonate analogs, a class of novel antivirals structurally related to natural nucleotides (Fig. 1). Cidofovir is a potent inhibitor of almost all types of DNA viruses (Hitchcock et al., 1996) and has been approved for treatment of cytomegalovirus retinitis in AIDS patients. Adefovir showed a strong in vitro effect against herpesviruses, hepadnaviruses, and retroviruses (Cihlar and Bischofberger, 1998). Its orally available prodrug is currently being evaluated as an anti-HIV agent in phase III clinical studies. In addition, clinical trials exploring the application of adefovir as a treatment for hepatitis B virus infections are under way.

Cidofovir and adefovir are actively secreted by the kidney (Cundy et al., 1995a,b), suggesting that active drug accumu-

---

ABBREVIATIONS: rROAT1, rat renal organic anion transporter 1; α-KG, α-ketoglutarate; bp, base; CKII, casein kinase II; EST, expressed sequence tag; hPAHT, human p-aminohippurate transporter; kb, kilobase pair; oatp, organic anion transporting polypeptide; OR-2, oocyte Ringer's 2; PAH, p-aminohippurate; PBS-M, phosphate-buffered saline/5% dry milk; PCR, polymerase chain reaction; PKA, protein kinase A; PKC, protein kinase C; PMEG, 9-(2-phosphonylmethoxyethyl)guanine; PMEDAP, 9-(2-phosphonylmethoxyethyl)diaminopurine; RT-PCR, reverse transcription-PCR; SSC, sodium chloride/sodium citrate solution; TK, tyrosine kinase; UTR, untranslated region; hOAT1, human renal organic anion transporter 1; mNKT(mROAT1), mouse renal organic anion transporter 1; fROAT1, winter flounder renal organic anion transporter 1.

lation in renal proximal tubules may play a role in the etiology of the drug-associated nephrotoxicity. In rabbits and rats, cidofovir is accumulated in kidney, reaching significantly higher concentration levels compared with other organs and tissues (Cundy et al., 1996a,b). Presumably, the uptake of cidofovir across the basolateral tubular membrane is more efficient than the subsequent secretion into tubular lumen resulting in drug accumulation in renal tubules. Hence, inhibition of the active drug uptake into proximal tubular cells may provide an effective strategy to ameliorate the renal toxicity syndromes. Previously this approach has been shown to be effective for some nephrotoxic β-lactam antibiotics. For example, *N*-benzoyl-β-alanine (betamipron) has been shown to reduce the nephrotoxicity of cephaloridine by inhibiting its tubular uptake (Tune, 1997). Similarly, in cynomolgus monkeys receiving chronic i.v. cidofovir treatment, coadministration of oral probenecid, an inhibitor of renal organic anion transport, reduced the incidence and severity of the drug-associated nephrotoxicity (Lacy et al., 1998b). Thus, identification and characterization of renal transporter(s) that mediate tubular uptake of cidofovir and/or adefovir would contribute to a better understanding of the mechanisms of their nephrotoxicity, as well as aid in the design of novel, specific, and effective nephroprotective agents.

The renal organic anion transport system, because of its sensitivity to probenecid and broad substrate specificity, is a primary candidate to mediate uptake of nucleoside phosphonate analogs into proximal tubules. Probenecid-sensitive renal organic anion transporters from rat (rROAT1/rOAT1), mouse [mNKT(mROAT1)], and winter flounder (fROAT1) have been previously cloned and characterized (Lopez-Nieto et al., 1997; Sekine et al., 1997; Sweet et al., 1997; Wolff et al., 1997). Upon expression in *Xenopus* oocytes, rROAT1 functions as an organic anion/dicarboxylate exchanger and mediates uptake of *p*-aminohippurate (PAH), cyclic nucleotides, and other small organic anions, indicating its broad substrate specificity (Sekine et al., 1997; Sweet et al., 1997). rROAT1 clearly represents the multispecific PAH/dicarboxylate exchanger previously detected by functional studies in basolateral membrane vesicles and isolated renal proximal tubules from a variety of species (Pritchard, 1988). In this study, we report the cloning and characterization of a human organic anion transporter, hOAT1, and demonstrate its function as a PAH/dicarboxylate exchanger. Importantly, we present data indicating that several antiviral nucleoside phosphonate analogs are high-affinity substrates for hOAT1 and that this transporter may be directly involved in mediating cidofovir- and adefovir-associated nephrotoxicity.

Materials and Methods

Screening of a Human Renal cDNA Library. A human kidney cDNA library was purchased from Invitrogen (Carlsbad, CA) and screened by colony hybridization with a 42-mer oligonucleotide (5′-CACTGCCGCCCGCCTGCCGATGCCAACCTCAGCAAGAACGGG-3′) corresponding to the 5′-end of clone expressed sequence tag (EST)58612 (GenBank accession number AA351032). The oligonucleotide was labeled with [^{32}P]dATP using T4 polynucleotide kinase. Bacterial colonies were transferred onto Hybond-N membranes (Amersham Pharmacia Biotech, Arlington Heights, IL) and hybridized overnight with the labeled probe in hybridization buffer (5× standard saline citrate (SSC), 5× Denhardt's solution, 0.05% SDS) at 68°C. Final washing was performed twice with 0.1× SSC + 0.1% SDS. Filters were subjected to autoradiography overnight, and several positive colonies were identified. Plasmid DNA was purified from these clones, and the length of their cDNA inserts determined by polymerase chain reaction (PCR).

DNA Sequencing and Analysis. The clone containing the largest cDNA insert (pOAT-8) was subjected to complete sequence analysis of both complementary strands by simultaneous "walking" from the 5′- and 3′-ends of the insert. Automatic sequencing was performed with Cy5-labeled oligonucleotide primers (Integrated DNA Technologies, Coralville, IA) using the Thermosequenase cycle sequencing kit (Amersham Pharmacia Biotech). All ambiguities were resolved by manual sequencing using the Thermosequenase radiolabeled terminator cycle sequencing kit (Amersham Pharmacia Biotech). If necessary, dideoxy-ITP was substituted for dideoxy-GTP to resolve sequence compressions. Initially, a BLAST search of the GenBank database identified mNKT(mROAT1) and rROAT1 as being related sequences, but no human homologs were found, and we designated this cDNA clone as hOAT1. All DNA and peptide sequence comparisons and database searches were done with the Wisconsin Package software (Genetics Computer Group, Madison, WI) with default settings.

Northern Blotting. A human multiple tissue Northern blot (CLONTECH, Palo Alto, CA) was used for localization of hOAT1 expression in human tissues. An hOAT1-specific [^{32}P]dATP-labeled probe was generated by random priming the *Bsr*GI/*Bsu*36I DNA fragment from pOAT-8 (nucleotides 420–854 of hOAT1 coding region). The membrane was hybridized for 1 h at 68°C in ExpressHyb hybridization buffer (CLONTECH) and then washed twice in 2× SSC with 0.05% SDS for 30 min at room temperature followed by a single wash in 0.1× SSC with 0.1% SDS at 50°C. The membrane was autoradiographed for 7 days at −70°C with intensifying screens. After stripping, the membrane was reprobed with a β-actin control probe provided by the manufacturer and autoradiographed for 3 h.

Tissue Localization by Reverse Transcription (RT)-PCR. The multiple choice cDNA kits I and II containing tissue-specific cDNAs (Origene Technologies, Rockville, MD) and two sets of hOAT1-specific primers were used for PCR detection of hOAT1 expression. The oligonucleotides, 5′-CCCGCTGGCACTCCTCCTCCGGGAG-3′ (sense), and 5′-GTAGAGCTCGGCAGTCATGCTCACCA-3′ (antisense), were used to amplify a 606-bp fragment from the hOAT1 coding region (nucleotides 815-1420). In the independent set of PCR reactions, a 295-bp hOAT1 fragment [composed of the last 175 coding nucleotides and 120 nucleotides of the 3′-untranslated region (UTR)] was amplified using the oligonucleotides, 5′-CCAGCGCTGTCACTGTCCTCCTGC-3′ (sense), and 5′-AACCCCCACACTTGGGTCACCATTTCCTC-3′ (antisense).

PCR reactions were carried out using the Expand High Fidelity PCR system (Roche Molecular Biochemicals) in a total volume of 25 μl containing 1 μg of tissue-specific cDNA. Thirty-five amplification cycles (95°C for 40 s, 58°C for 1 min, and 72°C for 45 s) were

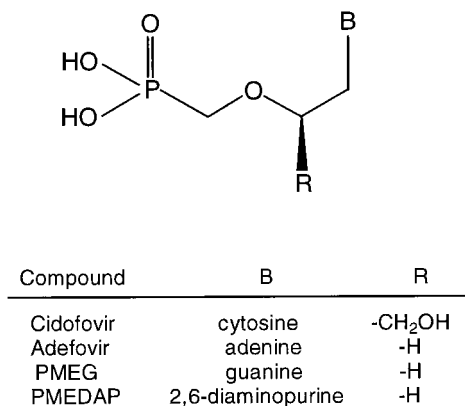| Compound	B	R
Cidofovir	cytosine	-CH$_2$OH
Adefovir	adenine	-H
PMEG	guanine	-H
PMEDAP	2,6-diaminopurine	-H

Fig. 1. Structure of acyclic nucleoside phosphonate analogs.

performed. A negative control without cDNA template was included in each set of reactions. As an internal control, a β-actin fragment was amplified using primers provided by the manufacturer.

In Vitro Expression of hOAT1. For efficient in vitro expression of hOAT1, the plasmid pOAT-8/ITT was constructed as follows. A fragment containing the first 500 bp of the hOAT1 coding region was amplified from pOAT-8 by the PCR using the sense primer 5′-ATGCCT<u>GGATCC</u>AAGCT<u>ATTTAGGTGACACTATAGAATACTCA</u>-<u>AGCTTGTTTTTTATTTTTAATTTTCTTTCAAATAC</u>GTCCACCAT-<u>GG</u>CCTTTAATGACC-3′ to introduce a *Bam*HI restriction site, the SP6 promoter, a truncated form of the 5′-UTR from alfalfa mosaic virus, and a favorable initiation context (these elements are underlined in the same order in the primer sequence). The oligonucleotide 5′-CGATGC-CTGGCCTTTGCCCATGGTCAGCTC-3′ was used as an antisense primer. The PCR product was digested with *Bam*HI and *Bsr*GI, and subcloned into *Bam*HI/*Bsr*GI-digested pOAT-8. Plasmid pOAT-8/ITT was expressed in vitro with the TNT SP6 Coupled Reticulocyte Lysate system (Promega, Madison, WI). A 25-μl reaction, containing 2 μg of circular plasmid and other components according to the manufacturer's protocol including complete amino acid mixture, was incubated for 2 h at 30°C and subjected to immunoblot analysis as described below.

Immunoblot Analysis of hOAT1. Rabbit anti-hOAT1 polyclonal antibody was prepared at AnaSpec (San Jose, CA) using standard immunological techniques. Briefly, a peptide corresponding to hOAT1 amino acids 515 to 528 was conjugated to keyhole limpet hemocyanine through a cysteine residue added to the C terminus of the peptide. Animal serum was collected after four immunizations in the presence of complete Freund's adjuvant and affinity-purified against the immunogenic peptide immobilized on a Sepharose resin.

For immunoblot analysis, human kidney cortex was obtained from the International Institute of Advanced Medicine (Exton, PA), frozen in liquid nitrogen, ground to a powder, and mixed with 10-fold excess (w/v) of extraction buffer (20 mM Tris-HCl, pH 7.5, 150 mM NaCl, 1% Nonidet P-40, 0.5% deoxycholate, 0.1% SDS). After homogenization in the presence of complete proteinase inhibitor cocktail (Roche Molecular Biochemicals) the extract was clarified by high-speed centrifugation. An aliquot was deglycosylated by incubation in the presence of peptide:*N*-glycosidase F (New England Biolabs, Beverly, MA) for 2 h at 37°C without prior denaturation. Tissue extracts (50 μg of protein) and in vitro expression reactions (10 μl) were separated by electrophoresis on an 8% SDS-polyacrylamide gel and electroblotted onto a nitrocellulose membrane (Millipore, Bedford, MA). The membrane was subsequently blocked in PBS/5% dry milk (PBS-M) for 1 h, washed three times in PBS/0.05% Tween 20, and incubated overnight in PBS-M with the anti-hOAT1 antibody. Following washing in PBS/0.05% Tween 20, the membrane was incubated in PBS-M with goat anti-rabbit antibody conjugated to horseradish peroxidase (Zymed, South San Francisco, CA). After an additional wash and incubation with a chemiluminescent substrate (Amersham Pharmacia Biotech), the immunoblot was exposed to X-ray film.

Xenopus Oocyte Expression Assay. For batch oocyte isolation, adult female *Xenopus laevis* (Xenopus One, Ann Arbor, MI) were anesthetized by hypothermia and decapitated. Ovaries were removed and divided into clumps of ~50 to 100 oocytes. Oocyte clumps were placed into a 50-ml conical tube containing oocyte Ringer's 2 (OR-2: 82.5 mM NaCl, 2.5 mM KCl, 1 mM Na_2HPO_4, 3 mM NaOH, 1 mM $CaCl_2$, 1 mM $MgCl_2$, 1 mM pyruvic acid, and 5 mM HEPES, pH 7.6) until they reached the 4-ml mark. Oocytes were rinsed three times with 10 ml of calcium-free OR-2 (82.5 mM NaCl, 2 mM KCl, 1 mM $MgCl_2$, and 5 mM HEPES, pH 7.6), placed in collagenase solution [5 mg/ml collagenase A (Roche Molecular Biochemicals) and 1 mg/ml trypsin inhibitor type III-O (Sigma Chemical Co., St. Louis, MO) in calcium-free OR-2] and swirled at 100 rpm for 2 to 2.5 h at 18°C. After collagenase treatment, the oocytes were rinsed five times with OR-2 containing 1 mg/ml BSA and placed in a phosphate/BSA solution for 1 h (100 mM K_2HPO_4 with 1 mg/ml BSA, pH 6.5). Oocytes were agitated every 15 min to remove the follicle and then rinsed five times with OR-2 + BSA. Stages V and VI oocytes were

collected and maintained at 18°C in OR-2 containing 0.05 mg/ml gentamycin sulfate, 2.5 mM sodium pyruvate, and 5% heat-inactivated horse serum. Overnight recovery was allowed before injection.

Capped cRNA for microinjection was synthesized from linearized plasmid DNA using Ambion's mMessage mMachine in vitro transcription kit (Ambion, Inc., Austin, TX). The cRNA products were quantitated in a spectrophotometer and diluted before injection to allow delivery of 20 ng of cRNA/oocyte in 16 nl with a 1- to 2-s injection.

Uptake assay was performed as described previously (Sweet et al., 1997). Briefly, 3 days after injection, the oocytes were divided into experimental groups (containing 10 oocytes each) and incubated at 18–22°C for 20 or 60 min in OR-2 containing various substrates in the absence or presence of inhibitors, as indicated in the figure legends. After uptake, oocytes were rapidly rinsed three times with ice-cold OR-2 and placed into individual scintillation vials containing 0.5 ml of 1 M NaOH, incubated at 65°C for 20 min, and neutralized with 0.5 ml of 1 M HCl. Finally, 4.7 ml of Ecolume (ICN Biomedical, Cleveland, OH) was added and radioactivity was determined in a Packard 1600TR liquid scintillation counter with external quench correction. Uptake was calculated in picomoles per oocyte.

Statistics. Data are presented as mean ± S.E. Differences in mean values were considered to be significant when $p \leq .05$ as determined by one-sample or paired Student's t test. The degree of significance was as indicated in the figure legends.

Chemicals. [^{3}H]PAH (3.7 Ci/mmol) was obtained from NEN Life Science Products (Boston, MA). [^{14}C]Tetraethylammonium (53 mCi/mmol) was obtained from American Radiolabeled Chemicals, Inc. (St. Louis, MO). Adefovir (30 Ci/mmol), cidofovir (56 mCi/mmol), [^{3}H]9-(2-phosphonylmethoxyethyl)guanine (PMEG; 34 Ci/mmol), and [^{3}H]9-(2-phosphonylmethoxyethyl)diaminopurine (PMEDAP; 32 Ci/mmol) were purchased from Moravek Biochemicals (Brea, CA). All unlabeled nucleoside phosphonates were synthesized at Gilead Sciences according to previously published procedures (Holy and Rosenberg, 1987). Unlabeled PAH, probenecid, and glutarate were obtained from Sigma.

Results

Cloning of hOAT1 cDNA. To identify potential cDNA sequences encoding a hOAT homolog, a BLAST search of the GenBank EST database was performed with the full-length rROAT1 cDNA sequence (Sweet et al., 1997). Two EST cDNA clones from human infant brain (accession number R25797 and AA351032), whose 5′-end regions exhibited a high level of sequence homology to rROAT1 between coding nucleotides 390 and 730, were identified. Therefore, an oligonucleotide probe derived from EST clone AA351032 was used to screen a human kidney cDNA library, and a positive clone was identified (pOAT-8). We refer to this cDNA clone as hOAT1.

Molecular Characterization of hOAT1. The complete DNA sequence of both strands of hOAT1 was determined, and the sense strand sequence is presented in Fig. 2A. The hOAT1 cDNA is 2118-bp long, including: 257 bp of 5′-UTR; a single, large open reading frame 1650-bp long; and 211 bp of 3′-UTR. The ATG at position 258 to 260 is the first start codon and has a correlation with Kozak's consensus for the translation initiation (Kozak, 1987) giving a predicted protein length of 550 amino acids with a molecular mass of 60.3 kDa. Hydropathy analysis (Kyte and Doolittle, 1982) predicted 12 potential α-helical membrane-spanning domains with both the amino and carboxyl termini located intracellularly (Fig. 2). According to this analysis, there is a large extracellular loop between transmembrane domains 1 and 2. Within this loop are five potential *N*-linked glycosylation

A.

```
-257 ....................................................................CTGCCCTGACCCCCAAAGTGAGGAGAAGCTGCAAGGGAAAAGG
-214 GAGGGACAGATCAGGCGAGACCGGGGAAGAAGGAGGAGCAGCCAAGGAGGCTGCTGTCCCCCCACAGAGCAGCTCGGACTCAGCTCCCGGAGCAACCCAGCTGCGGAG
-107 GCAACGGCAGTGCTGCTCCTCCAGCGAAGGACAGCAGGCAGGCAGACAGACGAGGTCCTGGGACTGGAAGGCCTCAGCCCCCAGCCACTGGGCTGGGCCTGGCCCA
```

```
   1 ATG GCC TTT AAT GAC CTC CTG CAG CAG GTG GGG GGT GTC GGC CGC TTC CAG CAG ATC CAG GTC ACC CTG GTG GTC CTC CCC
   1 Met Ala Phe Asn Asp Leu Leu Gln Gln Val Gly Gly Val Gly Arg Phe Gln Gln Ile Gln Val Thr Leu Val Val Leu Pro

  82 CTG CTC CTG ATG GCT TCT CAC AAC ACC CTG CAG AAC TTC ACT GCT GCC ATC CCT ACC CAC CAC TGC CGC CCG CCT GCC GAT
  28 Leu Leu Leu Met Ala Ser His Asn Thr Leu Gln Asn Phe Thr Ala Ala Ile Pro Thr His His Cys Arg Pro Pro Ala Asp
                                          *                                          ●

 163 GCC AAC CTC AGC AAG AAC GGG GGG CTG GAG GTC TGG CTG CCC CGG GAC AGG CAG GGG CAG CCT GAG TCC TGC CTC CGC TTC
  55 Ala Asn Leu Ser Lys Asn Gly Gly Leu Glu Val Trp Leu Pro Arg Asp Arg Gln Gly Gln Pro Glu Ser Cys Leu Arg Phe
          *                                                                              ●

 244 ACC TCC CCG CAG TGG GGA CTG CCC TTT CTC AAT GGC ACA GAA GCC AAT GGC ACA GGG GCC ACA GAG CCC TGC ACC GAT GGC
  82 Thr Ser Pro Gln Trp Gly Leu Pro Phe Leu Asn Gly Thr Glu Ala Asn Gly Thr Gly Ala Thr Glu Pro Cys Thr Asp Gly
                                      *                      *                              ●

 325 TGG ATC TAT GAC AAC AGC ACC TTC CCA TCT ACC ATC GTG ACT GAG TGG GAC CTT GTG TGC TCT CAC AGG GCC CTA CGC CAG
 109 Trp Ile Tyr Asp Asn Ser Thr Phe Pro Ser Thr Ile Val Thr Glu Trp Asp Leu Val Cys Ser His Arg Ala Leu Arg Gln
              *                                                          ●

 406 CTG GCC CAG TCC TTG TAC ATG GTG GGG GTG CTG CTC GGA GCC ATG GTG TTC GGC TAC CTT GCA GAC AGG CTA GGC CGC CGG
 136 Leu Ala Gln Ser Leu Tyr Met Val Gly Val Leu Leu Gly Ala Met Val Phe Gly Tyr Leu Ala Asp Arg Leu Gly Arg Arg

 487 AAG GTA CTC ATC TTG AAC TAC CTG CAG ACA GCT GTG TCA GGG ACC TGC GCA GCC TTC GCA CCC AAC TTC CCC ATC TAC TGC
 163 Lys Val Leu Ile Leu Asn Tyr Leu Gln Thr Ala Val Ser Gly Thr Cys Ala Ala Phe Ala Pro Asn Phe Pro Ile Tyr Cys

 568 GCC TTC CGG CTC CTC TCG GGC ATG GCT CTG GCT GGC ATC TCC CTC AAC TGC ATG ACA CTG AAT GTG GAG TGG ATG CCC ATT
 190 Ala Phe Arg Leu Leu Ser Gly Met Ala Leu Ala Gly Ile Ser Leu Asn Cys Met Thr Leu Asn Val Glu Trp Met Pro Ile

 649 CAC ACA CGG GCC TGC GTG GGC ACC TTG ATT GGC TAT GTC TAC AGC CTG GGC CAG TTC CTC CTG GCT GGT GTG GCC TAC GCT
 217 His Thr Arg Ala Cys Val Gly Thr Leu Ile Gly Tyr Val Tyr Ser Leu Gly Gln Phe Leu Leu Ala Gly Val Ala Tyr Ala

 730 GTG CCC CAC TGG CGC CAC CTG CAG CTA CTG GTC TCT GCG CCT TTT TTT GCC TTC TTC ATC TAC TCC TGG TTC TTC ATT GAG
 244 Val Pro His Trp Arg His Leu Gln Leu Leu Val Ser Ala Pro Phe Phe Ala Phe Phe Ile Tyr Ser Trp Phe Phe Ile Glu

 811 TCG GCC CGC TGG CAC TCC TCC TCC GGG AGG CTG GAC CTC ACC CTG AGG GCC CTG CAG AGA GTC GCC CGG ATC AAT GGG AAG
 271 Ser Ala Arg Trp His Ser Ser Ser Gly Arg Leu Asp Leu Thr Leu Arg Ala Leu Gln Arg Val Ala Arg Ile Asn Gly Lys
         ♦                                  ♦                              ♦

 892 CGG GAA GAA GGA GCC AAA TTG AGT ATG GAG GTA CTC CGG GCC AGT CTG CAG AAG GAG CTG ACC ATG GGC AAA GGC CAG GCA
 298 Arg Glu Glu Gly Ala Lys Leu Ser Met Glu Val Leu Arg Ala Ser Leu Gln Lys Glu Leu Thr Met Gly Lys Gly Gln Ala

 973 TCG GCC ATG GAG CTG CTG CGC TGC CCC ACC CTC CGC CAC CTC TTC CTC TGC CTC TCC ATG CTG TGG TTT GCC ACT AGC TTT
 325 Ser Ala Met Glu Leu Leu Arg Cys Pro Thr Leu Arg His Leu Phe Leu Cys Leu Ser Met Leu Trp Phe Ala Thr Ser Phe
         ■                                                      ♦

1054 GCA TAC TAT GGG CTG GTC ATG GAC CTG CAG GGC TTT GGA GTC AGC ATC TAC CTA ATC CAG GTG ATC TTT GGT GCT GTG GAC
 352 Ala Tyr Tyr Gly Leu Val Met Asp Leu Gln Gly Phe Gly Val Ser Ile Tyr Leu Ile Gln Val Ile Phe Gly Ala Val Asp

1135 CTG CCT GCC AAG CTT GTG GGC TTC CTT GTC ATC AAC TCC CTG GGT CGC CGG CCT GCC CAG ATG GCT GCA CTG CTG CTG GCA
 379 Leu Pro Ala Lys Leu Val Gly Phe Leu Val Ile Asn Ser Leu Gly Arg Arg Pro Ala Gln Met Ala Ala Leu Leu Leu Ala

1216 GGC ATC TGC ATC CTG CTC AAT GGG GTG ATA CCC CAG GAC CAG TCC ATT GTC CGA ACC TCT CTT GCT GTG CTG GGG AAG GGT
 406 Gly Ile Cys Ile Leu Leu Asn Gly Val Ile Pro Gln Asp Gln Ser Ile Val Arg Thr Ser Leu Ala Val Leu Gly Lys Gly

1297 TGT CTG GCT GCC TCC TTC AAC TGC ATC TTC CTG TAT ACT GGG GAA CTG TAT CCC ACA ATG ATC CGG CAG ACA GGC ATG GGA
 433 Cys Leu Ala Ala Ser Phe Asn Cys Ile Phe Leu Tyr Thr Gly Glu Leu Tyr Pro Thr Met Ile Arg Gln Thr Gly Met Gly

1378 ATG GGC AGC ACC ATG GCC CGA GTG GGC AGC ATC GTG AGC CCA CTG GTG AGC ATG ACT GCC GAG CTC TAC CCC TCC ATG CCT
 460 Met Gly Ser Thr Met Ala Arg Val Gly Ser Ile Val Ser Pro Leu Val Ser Met Thr Ala Glu Leu Tyr Pro Ser Met Pro

1459 CTC TTC ATC TAC GGT GCT GTT CCT GTG GCC GCC AGC GCT GTC ACT GTC CTC CTG CCA GAG ACC CTG GGC CAG CCA CTG CCA
 487 Leu Phe Ile Tyr Gly Ala Val Pro Val Ala Ala Ser Ala Val Thr Val Leu Leu Pro Glu Thr Leu Gly Gln Pro Leu Pro

1540 GAC ACG GTG CAG GAC CTG GAG AGC AGG AAA GGG AAA CAG ACG CGA CAG CAA CAA GAG CAC CAG AAG TAT ATG GTC CCA CTG
 514 Asp Thr Val Gln Asp Leu Glu Ser Arg Lys Gly Lys Gln Thr Arg Gln Gln Gln Glu His Gln Lys Tyr Met Val Pro Leu
         ■                                  ♦                                                          △

1621 CAG GCC TCA GCA CAA GAG AAG AAT GGA CTC TGA GGACTGAGAAGGGGCCTTACAGAACCCTAAAGGGAGGGAAGGTCCTACAGGTCTCCGGCCACC
 541 Gln Ala Ser Ala Gln Glu Lys Asn Gly Leu *
         ■

1717 CACACAAGGAGGAGGAAGAGGGAAATGGTGACCCAAGTGTGGGGGTTGTGGTTCAGGAAAGCATCTTCCCAGGGGTCCACCTCCCTTTATAAACCCCACCAGAACCAC
1824 ATCATTAAAAGGTTTGACTGCGAAAAAAAAAAAAAAAAA
```

Fig. 2. DNA and predicted amino acid sequence of hOAT1. A, complete nucleotide sequence of the sense strand of the hOAT1 cDNA and the predicted amino acid sequence of the single large open reading frame is shown. Approximate locations of the 12 predicted transmembrane domains are indicated below the peptide sequence by bars. Cysteine residues (●) and potential N-linked glycosylation sites (*) within the first extracellular loop are indicated. Potential intracellular phosphorylation sites for PKC (♦), CKII (■), and TK (△) are identified. Numbers to the left of the sequences indicate nucleotide and amino acid position, respectively. B, Kyte-Doolittle hydropathy plot. Proposed transmembrane domains are indicated by number.

B.

Kyte-Doolittle Plot

sites at Asn39, Asn56, Asn92, Asn97, and Asn113 and four cysteine residues at positions 49, 78, 105, and 128 that could participate in disulfide bond formation (Fig. 2A). A significant intracellular loop between transmembrane domains 6 and 7, from approximately amino acid residues 271 to 336, contains four protein kinase C (PKC) consensus sites located at Ser271, Ser278, Thr284, and Thr334 and a potential casein kinase II (CKII) site at Ser325 (Fig. 2A). Finally, within the carboxyl-terminal domain there is another putative PKC site at Thr521, two potential CKII sites at Thr515 and Ser543, and a tyrosine kinase consensus site at Tyr536. Whether any or all of these consensus sites participate in protein modification or function requires further experimentation.

During the course of our study, other reports have appeared in the literature concerning the cloning of hROATs designated hROAT1 (Reid et al., 1998), hOAT1–1 and hOAT1–2 (Hosoyamada et al., 1999), and human *p*-aminohippurate transporter (hPAHT) (Lu et al., 1999). Unfortunately, the DNA sequences for hOAT1–1 (accession number AB009697), hOAT1–2 (accession number AB009698), and hPAHT (no accession number reported) were not yet available in the GenBank database to compare with our hOAT1. Although there are some minor differences between our DNA sequence and that for hROAT1 (accession number AF057039), the predicted peptide sequence of our clone is identical with hROAT1 except for the final amino acid residue, Phe in hROAT1 versus Leu in hOAT1. At this time, no functional data has been published for hROAT1. Comparison with the published peptide sequence of hOAT1–2 confirms that our clone is the same, however, no characterization of hOAT1–2 was presented (Hosoyamada et al., 1999). Similarly, comparison with the published hPAHT sequence reveals that the sequence of our clone is identical except for the amino acid at position 14 (Ser in hPAHT versus Gly in hOAT1).

Alignment of the hOAT1 DNA sequence with hROAT1, rROAT1, mNKT(mROAT1), and fROAT showed a 99.7, 83.8, 83, and 59.5% identity, respectively. A summary of potential modification sites for these transporters is presented in Table 1. It is our opinion that hOAT1–2 and hPAHT have all of the same sites as those listed for hOAT1, yet, there was no mention of PKA, CKII, or tyrosine kinase (TK) consensus sites for hOAT1–2 (Hosoyamada et al., 1999) nor any CKII or TK sites for hPAHT (Lu et al., 1999). In contrast to our findings, Lu et al. (1999) reported four PKA consensus sites within the hPAHT

sequence, however, these sites do not conform to the consensus used in our motif search (R,K)2X(S,T).

Expression of hOAT1 in Human Tissues. Northern blot analysis was used to examine hOAT1 expression in different human tissues with an hOAT1-specific DNA probe. A strong signal was detected in kidney corresponding to a transcript 2.5-kb in size (Fig. 3a, top). In addition, there was a very weak signal of about 3.5 kb in liver that was detectable only after prolonged exposure. No positive signal was found in brain, heart, skeletal muscle, colon, thymus, spleen, small intestine, placenta, lung, or peripheral blood leukocytes. The lack of a detectable signal in brain was an unexpected result because, as mentioned above, two EST clones from a human infant brain cDNA library were identified with sequence identical to a 340-bp region of hOAT1. Therefore, we used the more sensitive technique of RT-PCR amplification to examine hOAT1 expression in various human tissues. Each sample was analyzed independently using two distinct sets of primers with proper negative controls (Fig. 3B, top and middle). A strong positive signal was consistently detected in kidney with both sets of primers. In contrast with the Northern analysis, RT-PCR amplification consistently yielded a product from brain. Interestingly, a strong positive signal was also detected in skeletal muscle, although only with one set of hOAT1-specific primers.

Immunoblot Analysis of hOAT1. A polyclonal antibody was generated in rabbits immunized with a synthetic peptide derived from a region of hOAT1 with predicted high antigenicity. In the immunoblot analysis of an extract from human kidney cortex, the antibody recognized a heterogeneous product with an apparent molecular mass of approximately 80 to 90 kDa (Fig. 4). This was significantly larger than the predicted molecular mass from the hOAT1 amino acid sequence. However, when the cortex extract was treated with peptide/*N*-glycosidase F, which specifically cleaves *N*-linked oligosaccharide chains, a 60-kDa homogeneous product was detected on the immunoblot. To determine whether this treatment completely removes all modifications from the hOAT1 peptide, we attempted to generate a control for the unmodified polypeptide by in vitro expression of hOAT1 cDNA in rabbit reticulocyte lysate. At first, no product of in vitro expression was detected in the presence of pOAT-8 plasmid. To achieve efficient expression, the original hOAT1 5′-UTR was replaced by a truncated form of the alfalfa mosaic virus RNA4

TABLE 1
Amino acid sequence motifs in renal organic anion transporter 1 homologs

Gene (species)	% Identity with hOAT1	Conserved cysteine residues	*N*-linked glycosylation consensus sites	Consensus sites			
				PKA	PKC	CKII	TK
hOAT1/ROAT1 (human)		**49, 78, 105, 128**	39, 56, 92, 97, 113		**Ser271, Ser278,** Thr284, Thr334, *Ser521*	**Ser325, Thr515,** Ser543	*Tyr536*
rROAT1/OAT1 (rat)	88	**49, 78, 105, 128**	39, 56, 92, 97, 113		**Ser271, Ser278,** Thr284, Thr334	**Ser325, Thr515,** Ser544	
mNKT (mROAT1) (mouse)	86	**49, 78, 99, 122**	39, 56, 86, 91, 107		**Ser265, Ser272,** Thr278, Thr328	**Ser319, Thr509,** Ser538	
fROAT (winter flounder)	49	**49, 81, 117, 140**	**54, 95,** 124	Thr351, Ser409	Thr13, Ser168, **Ser283, Ser290,** Ser324, Ser536, Ser543	**Ser337, Thr527,** Ser543, Thr549	

Potential modification sites for transport proteins with the corresponding amino acid position numbers within their respective polypeptide chains. Boldface denotes positions conserved between homologs, underline denotes positions conserved within mammals, and italics denotes sites unique to hOAT1.
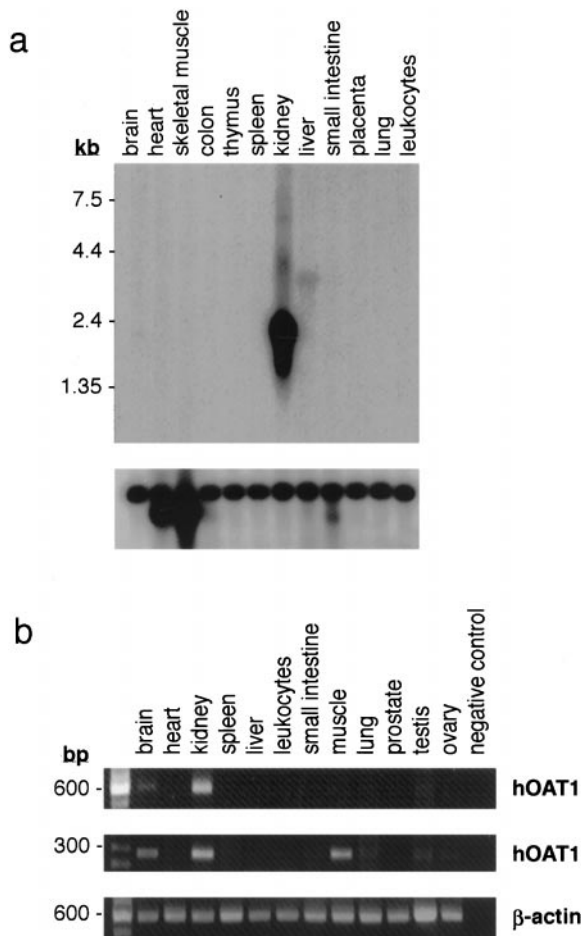
5'-UTR, which has been previously shown to significantly stimulate in vitro expression in reticulocyte lysate (Cihlar et al., 1997). In addition, the sequence surrounding the starting ATG codon was modified to match an optimal initiation context (Kozak, 1987). As shown in Fig. 4, the modified plasmid yielded a single polypeptide whose size was identical to that of the deglycosylated hOAT1. Together, these findings indicate that hOAT1 is modified by abundant *N*-glycosylation, which could account for up to 30% of its total molecular weight. Importantly, because all potential *N*-glycosylation sites reside within the large loop between the first and second putative transmembrane domain, it also shows that this loop is indeed located extracellularly as predicted from the hOAT1 hydropathy plot.

Functional Characterization of hOAT1 Transport. That the hOAT1 cDNA does indeed encode an organic anion transporter was confirmed by *Xenopus* oocyte expression assay. After cRNA injection, hOAT1-mediated uptake of 50 μM [^{3}H]PAH was equivalent to that seen with the previously identified basolateral organic anion transporter rROAT1 (Fig. 5; Sweet et al., 1997). Addition of 1 mM probenecid reduced PAH uptake by 98%, proving that virtually all of the

uptake was carrier mediated. Water-injected oocytes showed no appreciable uptake and were unaffected by probenecid.

The effects of various compounds and reduced temperature on hOAT1-mediated PAH uptake were also examined (Fig. 6). The organic anions probenecid, α-ketoglutarate (α-KG), bromcresol green, and 2,4-dichlorophenoxyacetic acid, as

Fig. 4. Immunoblot analysis of hOAT1. Samples were separated by electrophoresis on an 8% SDS-polyacrylamide gel, electroblotted onto nitrocellulose membrane, and probed with an hOAT1-specific polyclonal antibody followed by chemiluminescent detection. Kidney cortex extract before (lane 1) and after (lane 2) treatment with peptide/*N*-glycosidase F, and in vitro transcription/translation reaction in the presence (lane 3) and absence (lane 4) of pOAT-8/ITT plasmid.

Fig. 3. Detection of hOAT1 expression in human tissues. A, Northern analysis of human tissue-specific poly(A)+ RNA. After hybridization with a 430-bp, ^{32}P-labeled hOAT1 fragment, a 2.5-kb transcript was detected in kidney (top). The membrane was stripped and reprobed with a ^{32}P-labeled human β-actin-specific probe (bottom). B, analysis of hOAT1 tissue distribution using RT-PCR amplification of 606- and 295-bp hOAT1-specific regions (top and middle, respectively). As a control, a β-actin fragment was amplified from each tissue sample (bottom).

Fig. 5. Functional activity of hOAT1 in *Xenopus* oocytes. Three days after injection with rROAT1 or hOAT1 cRNA, oocytes were incubated in buffer containing 50 μM [^{3}H]PAH for 60 min, and uptake was determined in the absence (No Inhibitor) or presence (+ Inhibitor) of 1 mM probenecid. Data are mean ± S.E. values from a representative animal (10 oocytes/treatment).

well as excess unlabeled PAH, each reduced [³H]PAH uptake by at least 95% at 1 mM concentration. Interestingly, unlike the results reported for rROAT1 (Sweet et al., 1997), the organic anion urate (1 mM) was a fairly effective inhibitor of hOAT1, reducing PAH uptake by 75%; however, when used as substrate, there was no detectable transport of urate (data not shown). Transport was unaffected by the cation tetraethylammonium (1 mM) or by the P-glycoprotein inhibitor cyclosporin-A (10 μM). Furthermore, the ability of α-KG to *cis*-inhibit PAH uptake is indicative of a basolateral location for hOAT1, because the basolateral dicarboxylate/organic anion exchangers (e.g., rROAT1) should be inhibited by external α-KG as opposed to the luminal PAH carriers, which should be insensitive to this inhibition (Pritchard and Miller, 1993).

rROAT1 has been shown to function as a basolateral dicarboxylate/organic anion exchanger. If hOAT1 functions in the same way in human kidney, increasing the intracellular concentration of dicarboxylate should induce *trans*-stimulation of exogenous substrate uptake (Pritchard and Miller, 1993). For this determination, glutarate is the preferred counterion, because, in contrast to α-KG, it is not extensively metabolized (Pritchard, 1990). As shown in Fig. 7, incubating the oocytes in 5 mM glutarate for 90 min before exposure to PAH (i.e., preloading) significantly ($p < .0001$) stimulated PAH uptake in hOAT1-expressing oocytes, as compared with nonpreloaded oocytes. Moreover, glutarate preloading had no effect on water-injected oocytes (data not shown). Thus, glutarate induced *trans*-stimulation of hOAT1-mediated PAH uptake, suggesting that the uptake occurs in conjuction with the countertransport of dicarboxylate.

Nucleoside Phosphonate Analogs Are High-Affinity Substrates for hOAT1. Finally, the ability of rROAT1 and hOAT1 to mediate the transport of therapeutically important antiviral nucleoside phosphonates was tested. Together with adefovir (10 μM) and cidofovir (36 μM), two other nucleoside phosphonates with broad-spectrum antiviral and antiprolif-

erative activity, PMEG (10 μM) and PMEDAP (10 μM), were found to be substrates for both rROAT1 and hOAT1 (Fig. 8). However, uptake of all antivirals tested was markedly higher for hOAT1 compared with rROAT1. Little to no uptake was measured in water-injected oocytes, indicating the complete lack of diffusive uptake of these nucleotide analogs. Like PAH, both hOAT1- and rROAT1-mediated uptake of all nucleoside phosphonates was efficiently blocked by 1 mM probenecid. In contrast to hOAT1 and rROAT1, the renal organic cation transporter 2, did not mediate detectable uptake of adefovir or cidofovir in renal organic cation transporter 2 cRNA-injected oocytes (data not shown). Finally, similar to PAH, preloading the oocytes in 5 mM glutarate for 90 min before exposure to adefovir significantly stimulated adefovir uptake in rROAT1 (5.3-fold increase, $p < .001$) and hOAT1 (1.5-fold increase, $p < .01$)-expressing oocytes, as compared with nonpreloaded oocytes. Thus, hOAT1-mediated adefovir uptake correlates with the countertransport of dicarboxylate.

To find out whether the marked dissimilarity between rROAT1 and hOAT1 transport of nucleoside phosphonates is simply due to different levels of expression of the two transporters or actually due to lower substrate affinity of rROAT1, K_m values for cidofovir and adefovir were determined. Adefovir and cidofovir uptake by hOAT1-expressing oocytes increased steadily with time and was linear for about 1 h (data not shown). Using a 20-min incubation period to approximate initial rate, the transport was assessed by incubating cRNA-injected oocytes in medium containing 0.002 to 1 mM substrate concentrations. Double reciprocal plots of the saturation data were constructed, and linear regression analysis was performed to obtain K_m estimates (Fig. 9). Adefovir and cidofovir exhibited K_m values of 30 and 46 μM, respectively, for hOAT1-mediated transport (Table 2). However, the corresponding K_m values for rROAT1-mediated transport were 5- and 9-fold higher, respectively, compared with hOAT1. A significant difference in K_m values between the two transporters was also observed for PAH (Table 2).
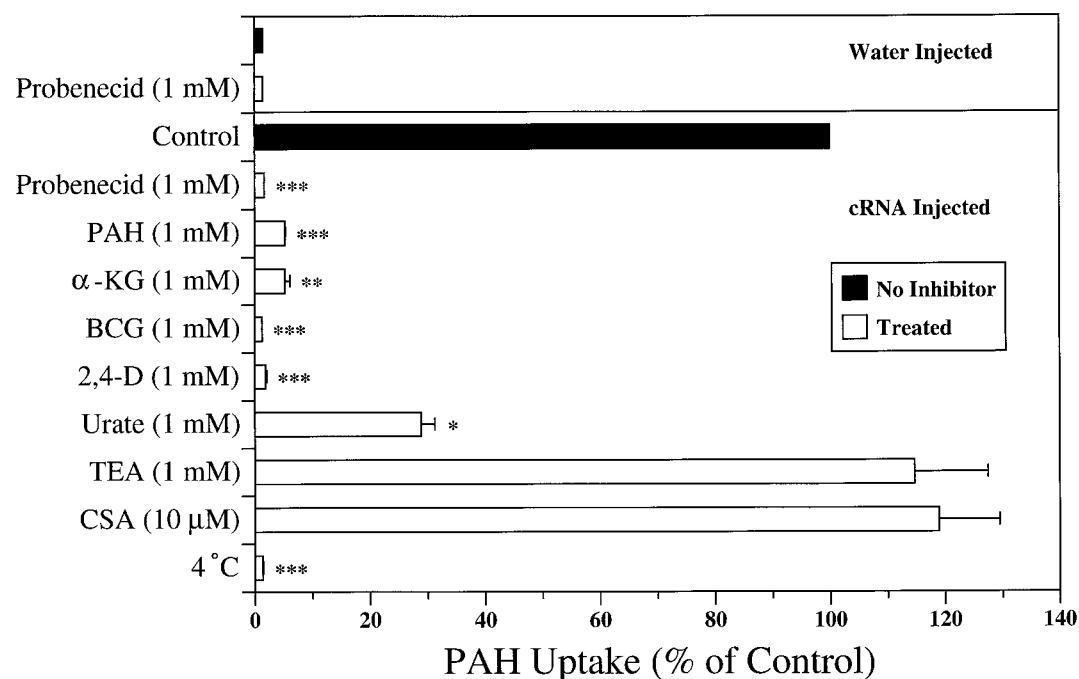
Fig. 6. Inhibition profile of hOAT1-mediated PAH uptake. cRNA from hOAT1 was injected into oocytes, and 50 μM [³H]PAH transport was measured after 60 min in the presence of several organic anions and cations. Data are presented as percentage of control uptake. Values are mean $\pm$ S.E. for two animals (10 oocytes/treatment/animal). *$p \leq$ .05, **$p \leq$ .01, and ***$p \leq$ .001, as determined by one sample Student's t test.
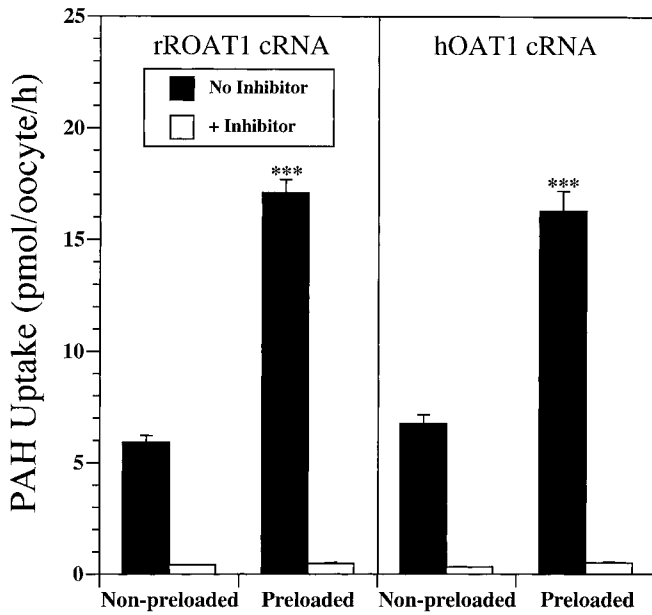
Fig. 7. *trans*-Stimulation of rROAT1- and hOAT1-mediated uptake. rROAT1 or hOAT1 cRNA-injected oocytes, either nonpreloaded or preloaded by 90 min of incubation in 5 mM glutarate, were washed with glutarate-free medium and exposed to 50 μM [^{3}H]PAH for 60 min in the absence (No Inhibitor) or presence (+ Inhibitor) of 1 mM probenecid. There was no effect on similarly treated water-injected oocytes (data not shown). Data are mean $\pm$ S.E. values from two animals (10 oocytes/ treatment/animal). ***$p \leq .001$, as determined by paired Student's t test.

Discussion

Besides other important functions, the kidney plays an indispensable role in maintaining body homeostasis, and it is highly specialized for this purpose. Its functional unit, the nephron, is a polarized epithelium equipped with transport systems that mediate active secretion and/or reabsorption of a variety of small molecules. For drugs and other foreign compounds, secretion is achieved through coordinated function of basolateral and apical transporters operating in series (Pritchard and Miller, 1993). The elimination of some drugs and xenobiotics is so effective that they are completely cleared from renal plasma in a single pass through the kidney. Because the kidney handles one-fifth of the entire cardiac output, proximal tubular epithelium must possess a remarkable transport capacity. This has a significant implication for drug therapy, because the secretory transport may lead to an active drug accumulation within proximal tubular cells with associated risk of nephrotoxicity. Animal toxicology and pharmacokinetic studies suggested that such mechanisms may also be involved in the nephrotoxicity induced by cidofovir and adefovir therapy. In this study, we have cloned and expressed hOAT1 and shown that it exhibits a high affinity toward these clinically important antivirals.

The clone hOAT1 is virtually identical with a human clone identified as hROAT1 by Reid et al. (1998), differing only in the terminal amino acid, Phe in hROAT1 versus Leu in hOAT1. Notably, Leu has been reported as the final amino
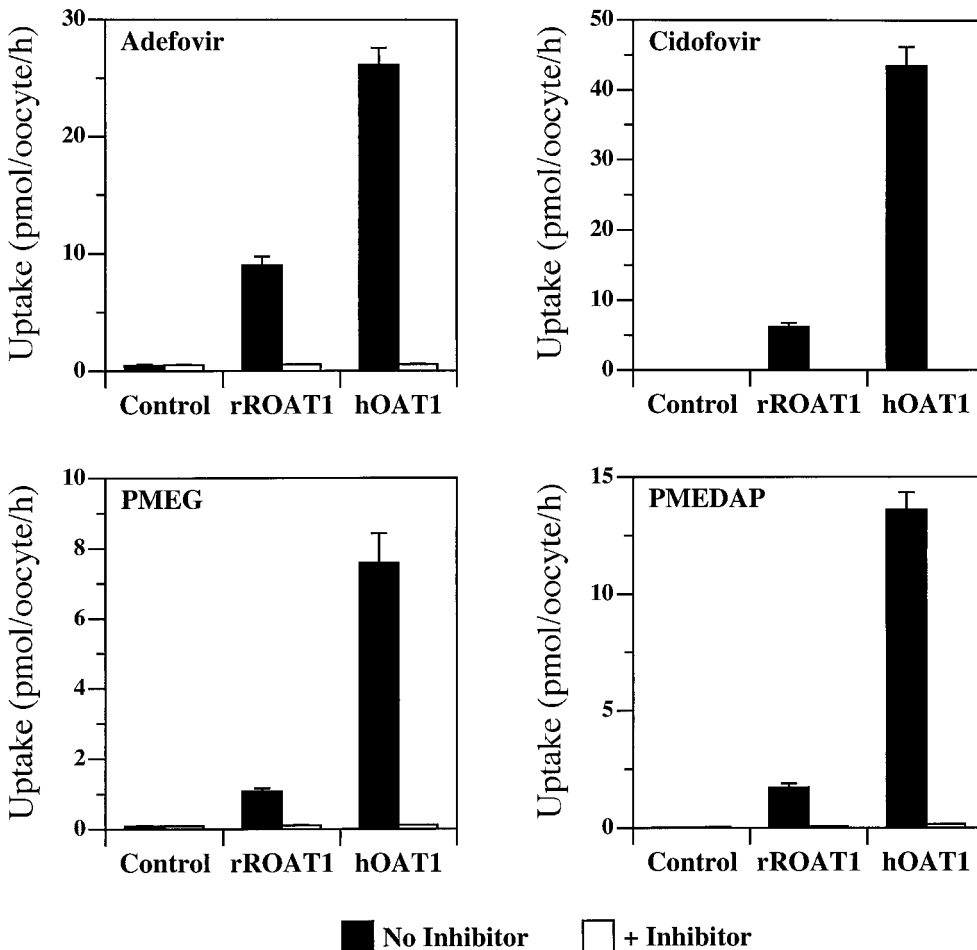
Fig. 8. Uptake of antiviral nucleoside phosphonates mediated by hOAT1 and rROAT1. *Xenopus* oocytes were injected with hOAT1 or rROAT1 cRNA, and substrate accumulation was determined in the absence (No inhibitor) or presence (+ Inhibitor) of 1 mM probenecid. Substrate concentrations were as follows: 10 μM adefovir, 36 μM cidofovir, 10 μM PMEG, and 10 μM PMEDAP. Data are mean $\pm$ S.E. values from representative animals (10 oocytes/treatment/animal).

acid in rROAT1, mNKT(mROAT1), hOAT1–1, hOAT1–2, and hPAHT. The recent study by Lu et al. (1999) describes the isolation of hPAHT, which differs from hOAT1 at position 14 (Gly in hOAT1 versus Ser in hPAHT). In this instance, rROAT1, mNKT(mROAT1), hOAT1–2, hROAT1, and even
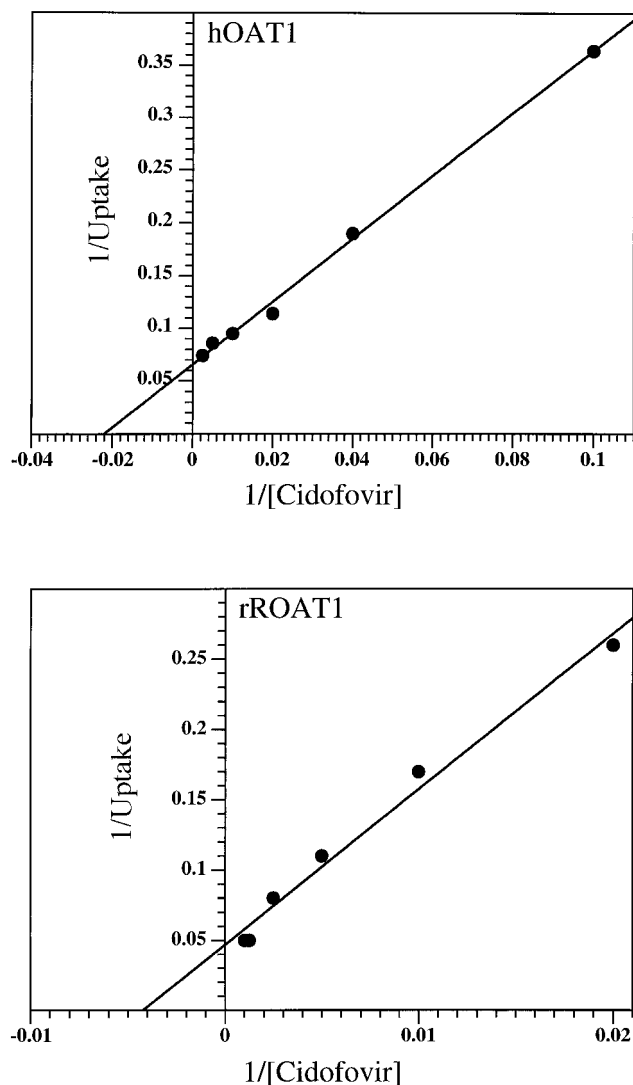
Fig. 9. Kinetic analysis of hOAT1- and rROAT1-mediated transport of cidofovir. hOAT1 and rROAT1 cRNA-injected oocytes were exposed to increasing substrate concentrations (0.002 to 1 mM depending on substrate and transporter) for 20 min. Saturation analysis was performed, and a representative double reciprocal plot with linear regression analysis is shown. The determined K_m values for all of the substrates tested are reported in Table 2. The data shown are mean ± S.E. values from three to four animals (10 oocytes/treatment/animal).

TABLE 2

Comparison of hOAT1 and rROAT1 substrate affinity

Substrate	hOAT1	rROAT1
	$K_m \, \mu M$	
Cidofovir	46	238
Adefovir	30	270
PAH	4	70

Each K_m was determined from a double reciprocal plot of a 20-min uptake at substrate concentrations ranging from 10 to 400 μM for hOAT1 (PAH was 2 to 20 μM because of its lower K_m) and 50 to 1000 μM for rROAT1. Plotted data were mean ± S.E. values from three to four animals (10 oocytes/concentration/animal), and K_m values were rounded to the nearest whole number. K_m data of PAH for rROAT1 are reproduced from Sweet et al., 1997.

fROAT, all have Gly at position 14. These two sequence differences may be the result of PCR errors introduced by the method used to clone hROAT1 and hPAHT. hOAT1 also appears to be the same clone as that designated as hOAT1–2 by Hosoyamada et al. (1999). However, the transport properties of hOAT1–2 were not characterized in the study. Finally, a fourth closely related human clone was designated as hOAT1–1 by Hosoyamada et al. (1999), which differs from hOAT1–2 by an extra 13 amino acid stretch in the C terminus.

The presence of hOAT1-specific mRNA was detected in human kidney as well as brain when the sensitive technique of RT-PCR amplification was used. Similarly, presence of mouse OAT1/NKT-specific mRNA has been localized to kidney as well as brain (Lopez-Nieto et al., 1997). However, although organic anion transport activity has been previously detected in choroid plexus (Miller and Ross, 1976), presence of hOAT1 protein as well as its precise localization and function in brain remains to be elucidated.

Characterization of hOAT1 in *Xenopus* oocytes indicated that, like rROAT1, it functions as a PAH/dicarboxylate exchanger. Specifically, it mediates PAH accumulation, which was effectively inhibited by a variety of organic anions, including urate (although urate itself was not a substrate). Importantly, substrate uptake into oocytes was *trans*-stimulated by glutarate, indicating that hOAT1 mediates dicarboxylate/organic anion exchange (Fig. 7). This is consistent with a role of hOAT1 in basolateral uptake of anionic drugs from the plasma, as previously established for rROAT1 (Pritchard, 1988; Sekine et al., 1997; Sweet et al., 1997). However, it must be noted that unlike rat kidney, the human kidney appears capable of dicarboxylate/organic anion exchange at luminal as well as basolateral membranes (Roch-Ramel et al., 1996). Kidney tissue immunostaining revealed predominant, if not exclusive, localization of hOAT1–1 in the basolateral membrane of the proximal tubule (Hosoyamada et al., 1999). However, in either location, basolateral or apical, the in vivo orientation of the dicarboxylate gradient (in > out) (Pritchard and Miller, 1993) dictates that hOAT1 must mediate cellular uptake of its exogenous substrates.

We showed that four antiviral nucleoside phosphonate analogs were substrates for hOAT1 (Table 2 and Fig. 8). Interestingly, hOAT1 has significantly higher affinity to nucleoside phosphonates compared with rROAT1. This may explain, in part, the observation that a higher dose of adefovir is required to induce nephrotoxicity syndromes in rats (Lacy et al., 1998a) compared with humans (Fisher et al., 1999). If hOAT1 is involved in cidofovir- and/or adefovir-associated nephrotoxicity, these drugs should show their highest renal accumulation in those segments of the proximal tubule expressing the organic anion/dicarboxylate exchanger. In rabbits, PAH/dicarboxylate transport activity is most abundantly expressed in the S2 segment of proximal tubule (Shpun et al., 1995). Furthermore, in situ hybridization using a specific cRNA probe demonstrated high levels of rROAT1 expression in the S2 segment of rat renal proximal tubules (Sekine et al., 1997). Notably, rabbits show the highest accumulation of cidofovir in the most superficial part of cortex (Cundy et al., 1996b), which contains S1 and S2 proximal tubular segments, suggesting that cidofovir accumulation does colocalize with expression of the basolateral organic anion/dicarboxylate exchanger (i.e., rROAT1 and by infer-

ence, hOAT1). In addition, clinical pharmacokinetic studies demonstrated that the peak plasma drug levels (C_{max}) generated by therapeutically relevant doses of cidofovir and adefovir are 30 to 40 μM (Cundy et al., 1995b) and 0.5 to 1 μM (Barditch-Crovo et al., 1997), respectively, suggesting that tubular uptake of the two antivirals may proceed below saturation of hOAT1. However, it should be noted that *Xenopus* oocytes may exhibit a somewhat unique pattern of posttranslational modifications, which could result in some functional differences between the native and expressed hOAT1. Therefore, it would be important to study hOAT1 in a more relevant, e.g., mammalian, expression system to confirm the suggested relationship between pharmacokinetics and tubular transport of adefovir and cidofovir. Nevertheless, the findings discussed above argue that hOAT1 can mediate active accumulation of nucleoside phosphonates in human proximal tubules and, thus, may be directly involved in the etiology of cidofovir-and/or adefovir-associated nephrotoxicity.

Besides hOAT1, other renal transporters may also potentially contribute to active tubular accumulation of these drugs. Among others, recently identified rat organic anion transporting polypeptide (oatp) type 3 is expressed almost exclusively in kidney, and transports organic anions like thyroxine or taurocholic acid (Abe et al., 1998). Closely related rat oatp-1 and its human homolog are expressed in liver, as well as in kidney, and transport steroid hormones, sulfobromophthalein, and other organic anions (Jacquemin et al., 1994; Kullak-Ublick et al., 1995). Another renal transporter OAT-K1 transports folate, methotrexate, and nonsteroidal anti-inflammatory drugs (Saito et al., 1996). Some structural similarity was found between OAT-K1, oatp-1, and oatp-3 (Jacquemin et al., 1994; Kullak-Ublick et al., 1995; Saito et al., 1996; Abe et al., 1998). Accordingly, they all exhibit low sensitivity to probenecid and are unable to transport PAH. On the contrary, rOAT-2 expressed in liver and kidney is more likely to recognize nucleoside phosphonates because of its broad substrate specificity, which includes PAH and α-KG (Sekine et al., 1998).

In addition to uptake across the basolateral membrane, efflux across the apical membrane should also influence the steady-state tubular accumulation of nucleoside phosphonates. The accumulation of nucleoside phosphonates in kidney cortex suggests that the luminal efflux is presumably the rate-limiting step in their tubular secretion pathway (Cundy et al., 1996a,b). To date, it is not clear how the apical efflux of PAH functions and whether nucleoside phosphonates share this route with PAH. There are some suggestions that PAH/α-KG exchanger may be present in human renal apical tubular membrane (Roch-Ramel, 1998). However, its relation to hOAT1 remains to be elucidated. Notably, multidrug resistance-associated protein, which mediates ATP-dependent efflux of hydrophobic anions, has been detected in the apical membrane of kidney proximal tubules (Schaub et al., 1997), suggesting that it may be a potential candidate for mediating apical efflux of nucleoside phosphonates.

In summary, we cloned and characterized a human renal organic anion transporter and identified several novel substrates among a class of clinically important antivirals. Further characterization of the substrate specificity of hOAT1 may help to identify new potentially nephrotoxic agents. In addition, progress in elucidation of the structure/function relationships of hOAT1, including identification of its sub-strate/inhibitor binding domains, will be invaluable toward the rational design of novel, specific, and potent inhibitors that may serve as efficient nephroprotectants.

References

Abe T, Kakyo M, Sakagami H, Tokui T, Nishio T, Tanemoto M, Nomura H, Hebert SC, Matsuno S, Kondo H and Yawo H (1998) Molecular characterization and tissue distribution of a new organic anion transporter subtype (oatp3) that transports thyroid hormones and taurocholate and comparison with oatp2. *J Biol Chem* **273:**22395–22401.

Barditch-Crovo P, Toole J, Hendrix CW, Cundy KC, Ebeling D, Jaffe HS and Lietman PS (1997) Anti-human immunodeficiency virus (HIV) activity, safety, and pharmacokinetics of adefovir dipivoxil (9-[2-(bis-pivaloyloxymethyl)phosphonyl-methoxyethyl]adenine) in HIV-infected patients. *J Infect Dis* **176:**406–413.

Carr A, Samaras K, Burton S, Law M, Freund J, Chisholm DJ and Cooper DA (1998) A syndrome of peripheral lipodystrophy, hyperlipidaemia and insulin resistance in patients receiving HIV protease inhibitors. *AIDS* (*London*) **12:**F51–F58.

Cihlar T and Bischofberger N (1998) PMEA and PMPA: Acyclic nucleoside phosphonates with potent anti-HIV activity, in *Trends in Drug Research II* (Van der Goot H ed) pp 105–116, Elsevier, Amsterdam.

Cihlar T, Fuller MD and Cherrington JM (1997) Expression of the catalytic subunit (UL54) and the accessory protein (UL44) of human cytomegalovirus DNA polymerase in a coupled *in vitro* transcription/translation system. *Protein Expr Purif* **11:**209–218.

Cundy KC, Barditch-Crovo P, Walker RE, Collier AC, Ebeling D, Toole J and Jaffe HS (1995a) Clinical pharmacokinetics of adefovir in human immunodeficiency virus type 1-infected patients. *Antimicrob Agents Chemother* **39:**2401–2405.

Cundy KC, Petty BG, Flaherty J, Fisher PE, Polis MA, Wachsman M, Lietman PS, Lalezari JP, Hitchcock MJM and Jaffe HS (1995b) Clinical pharmacokinetics of cidofovir in human immunodeficiency virus-infected patients. *Antimicrob Agents Chemother* **39:**1247–1252.

Cundy KC, Bidgood AM, Lynch G, Shaw JP, Griffin L and Lee WA (1996a) Pharmacokinetics, bioavailability, metabolism, and tissue distribution of cidofovir (HPMPC) and cyclic HPMPC in rats. *Drug Metab Dispos* **24:**745–752.

Cundy KC, Li ZH and Lee WA (1996b) Effect of probenecid on the distribution, metabolism, and excretion of cidofovir in rabbits. *Drug Metab Dispos* **24:**315–321.

Dalakas M, Illa I, Pezeshkpour GH, Laukaitis JP, Cohen B and Griffin JL (1990) Mitochondrial myopathy caused by long-term AZT (zidovudine) therapy: Management and differences from HIV-associated myopathy. *N Engl J Med* **322:**1098–1105.

Dubinsky RM, Yarchoan R, Dalakas M and Broder S (1989) Reversible azonal neuropathy from the treatment of AIDS and related disorders with 2′,3′-dideoxycytidine (ddC). *Muscle Nerve* **12:**856–860.

Fisher E, Brosgart C, Cohn D, Chaloner K, Pulling C, Scmetter B, Alston B and El-Sadr W (1999) Safety of adefovir dipivoxil (ADV) and incidence of proximal renal tubular disorder (PRTD) in a placebo-controlled trial in patients with advanced HIV disease (Abstract). *6th Conference on Retroviruses and Opportunistic Infections*, Abstract no. 491, p 160; Chicago. Alexandria, VA: Foundation for Retrovirology and Human Health.

Hitchcock MJM, Jaffe JS, Martin JC and Stagg RJ (1996) Cidofovir, a new agent with potent anti-herpesvirus activity. *Antiviral Chem Chemother* **7:**115–127.

Holy A and Rosenberg I (1987) Synthesis of 9-(2-phosphonylmethoxyethyl)adenine and related compounds. *Collect Czech Chem Commun* **52:**2801–2809.

Hosoyamada M, Sekine T, Kanai Y and Endou H (1999) Molecular cloning and functional expression of a multispecific organic anion transporter from human kidney. *Am J Physiol* **276:**F122–F128.

Jacquemin E, Hagenbuch B, Stieger B, Wolkoff AW and Meier PJ (1994) Expression cloning of a rat liver Na(+)-independent organic anion transporter. *Proc Natl Acad Sci USA* **91:**133–137.

Kozak M (1987) An analysis of 5′-noncoding sequences from 699 vertebrate messenger RNAs. *Nucleic Acids Res* **15:**8125–8148.

Kullak-Ublick GA, Hagenbuch B, Stieger B, Schteingart CD, Hofmann AF, Wolkoff AW and Meier PJ (1995) Molecular and functional characterization of an organic anion transporting polypeptide cloned from human liver. *Gastroenterology* **109:**1274–1282.

Kyte J and Doolittle RF (1982) A simple method for displaying the hydropathic character of a protein. *J Mol Biol* **157:**105–132.

Lacy SA, Hitchcock MJM, Lee WA, Taylor A, Eisenberg G and Cundy KC (1998a) Evaluation of toxicity associated with chronic administration of anti-HIV nucleotide analogue adefovir dipivoxil in rats and cynomolgus monkeys (Abstract). *Society of Toxicology Meeting*, Abstract no. 1844, p 283; Seattle. Reston, VA: Society of Toxicology.

Lacy SA, Hitchcock MJM, Lee WA, Tellier P and Cundy KC (1998b) Effect of oral probenecid coadministration on the chronic toxicity and pharmacokinetics of intravenous cidofovir in cynomolgus monkeys. *Toxicol Sci* **4:**97–106.

Lalezari JP, Stagg RJ, Kuppermann BD, Holland GN, Kramer F, Ives DV, Youle M, Robinson MR, Drew WL and Jaffe HS (1997) Intravenous cidofovir for peripheral cytomegalovirus retinitis in patients with AIDS: A randomized, controlled trial. *Ann Intern Med* **126:**257–263.

Lopez-Nieto CE, You G, Bush KT, Barros EJ, Beier DR and Nigam SK (1997) Molecular cloning and characterization of NKT, a gene product related to the organic cation transporter family that is almost exclusively expressed in the kidney. *J Biol Chem* **272:**6471–6478.

Lu R, Chan BS and Schuster VL (1999) Cloning of the human kidney PAH transporter: Narrow substrate specificity and regulation by protein kinase C. *Am J Physiol* **276:**F295–F303.

Miller TB and Ross CR (1976) Transport of organic cations and anions by choroid plexus. *J Pharmacol Exp Ther* **196:**771–777.

Pritchard JB (1988) Coupled transport of *p*-aminohippurate by rat kidney basolateral membrane vesicles. *Am J Physiol* **255:**F597–F604.

Pritchard JB (1990) Rat renal cortical slices demonstrate *p*-aminohippurate/ glutarate exchange and sodium/glutarate coupled *p*-aminohippurate transport. *J Pharmacol Exp Ther* **255:**969–975.

Pritchard JB and Miller DS (1993) Mechanisms mediating renal secretion of organic anions and cations. *Physiol Rev* **73:**765–796.

Reid G, Wolff NA, Dautzenberg FM and Burckhardt G (1998) Cloning of a human renal *p*-aminohippurate transporter, hROAT1. *Kidney Blood Press Res* **21:**233–237.

Roch-Ramel F, Guisan B and Schild L (1996) Indirect coupling of urate and *p*-aminohippurate transport to sodium in human brush-border membrane vesicles. *Am J Physiol* **270:**F61–F68.

Roch-Ramel F (1998) Renal transport of organic anions. *Curr Opin Nephrol Hypertens* **7:**517–524.

Saito H, Masuda S and Inui K (1996) Cloning and functional characterization of a novel rat organic anion transporter mediating basolateral uptake of methotrexate in the kidney. *J Biol Chem* **271:**20719–20725.

Schaub TP, Kartenbeck J, Konig J, Vogel O, Witzgall R, Kriz W and Keppler D (1997) Expression of the conjugate export pump encoded by the mrp2 gene in the apical membrane of kidney proximal tubules. *J Am Soc Nephrol* **8:**1213–1221.

Sekine T, Watanabe N, Hosoyamada M, Kanai Y and Endou H (1997) Expression cloning and characterization of a novel multispecific organic anion transporter. *J Biol Chem* **272:**18526–18529.

Sekine T, Cha SH, Tsuda M, Apiwattanakul N, Nakajima Y and Endou H (1998) Identification of multispecific organic anion transporter 2 expressed predominantly in the liver. *FEBS Lett* **429:**179–182.

Shpun S, Evans KK and Dantzler WH (1995) Interaction of alpha-KG with basolateral organic anion transporter in isolated rabbit renal S3 proximal tubules. *Am J Physiol* **268:**F1109–F1116.

Sweet DH, Wolff NA and Pritchard JB (1997) Expression cloning and characterization of ROAT1, the basolateral organic anion transporter in rat kidney. *J Biol Chem* **272:**30088–30095.

Tune BM (1997) Nephrotoxicity of beta-lactam antibiotics: Mechanisms and strategies for prevention. *Pediatr Nephrol* **11:**768–772.

Wolff NA, Werner A, Burkhardt S and Burckhardt G (1997) Expression cloning and characterization of a renal organic anion transporter from winter flounder. *FEBS Lett* **417:**287–291.